Polymer 50 (2009) 1456–1462

Contents lists available at ScienceDirect

Polymer

journal homepage: www.elsevier.com/locate/polymer

A study of thermoassociative gelation of aqueous cationic poly(*N*-isopropyl acrylamide) graft copolymer solutions

R. Liu [a,b], F. Cellesi [c], N. Tirelli [c], B.R. Saunders [a,*]

[a] *Polymer Science and Technology Group, The School of Materials, The University of Manchester, Grosvenor Street, Manchester M1 7HS, UK*
[b] *School of Material and Chemical Engineering, Zhengzhou University of Light Industry, Zhengzhou 450002, P.R. China*
[c] *Laboratory of Polymers and Biomaterials, School of Pharmacy, The University of Manchester, Oxford Road, Manchester M13 9PT, UK*

ARTICLE INFO

Article history:
Received 9 November 2008
Received in revised form
14 January 2009
Accepted 15 January 2009
Available online 23 January 2009

Keywords:
Thermoassociative gel formation
Cationic PNIPAm graft copolymer
Dynamic rheology

ABSTRACT

In this work thermoassociative gel formation of a new family of aqueous temperature-responsive copolymer solutions has been investigated. This was achieved using a cationic poly(*N*-isopropyl acrylamide) (PNIPAm) graft copolymer recently prepared [Liu R, De Leonardis P, Cellesi F, Tirelli N, Saunders BR. *Langmuir* 2008;24:7099]. The $PDMA^{+}{}_{x}$-*g*-$(PNIPAm_{n})_{y}$ copolymers have *x* and *y* values that originate from the macroinitiator; the value for *n* corresponds to the PNIPAm arm length. DMA^{+} is quarternarized *N*,*N*-dimethylaminoethyl methacrylate. The copolymer solutions exhibited cloud point temperatures (T_{clpt}) of about 33 °C, which were not significantly affected by *x*/*y* ratio or the value for *n*. Thermoassociative gel formation occurred above T_{clpt} at copolymer concentrations (C_{copol}) greater than or equal to 4 wt.%. This is a reasonably low C_{copol} value and is a consequence of the graft copolymer architecture employed. We investigated the effect of temperature, C_{copol} and copolymer structure on gelation and gel elasticity using variable – temperature dynamic rheology. For $PDMA^{+}{}_{30}$-*g*-$(PNIPAm_{210})_{14}$ solutions at 39 °C it was found that G' (elastic modulus) scales with C_{copol} according to $G' \sim C_{copol}^{3.85}$. The data suggested that a significant proportion of PNIPAm units is not directly involved in network formation. Thermoassociative gel formation and the gel properties for these systems appear to be governed by a balance between electrostatic repulsion involving the DMA^{+} units (favouring spatial extension of the copolymer backbones) and attractive hydrophobic interactions between PNIPAm side chains (favouring associative crosslink formation).

1. Introduction

In previous work [1] we introduced a new temperature-responsive family of cationic graft copolymers, $PDMA^{+}{}_{x}$-*g*-$(PNIPAm_{n})_{y}$. DMA^{+} and NIPAm are quarternarized *N*,*N*-dimethylaminoethyl methacrylate and *N*-isopropylacrylamide, respectively. That study involved a comprehensive investigation of dilute dispersion behaviour. These copolymers are potentially of significant interest because they can adsorb to anionic dispersions and confer responsive behaviour to them [2]. Our copolymers are architecturally unique compared to other thermoassociative copolymers [3–6] because they are cationic graft copolymers. They were constructed using atom transfer radical polymerization (ATRP). Thermoassociation of the $PDMA^{+}{}_{x}$-*g*-$(PNIPAm_{n})_{y}$ chains occurs [1] at or above the cloud point temperature (T_{clpt}). However, the gelation temperatures have not yet been determined in the absence of shear and the factors governing the elasticity of the gels have not been investigated. In this study we extend our previous work to sensitively probe gel formation and properties using dynamic rheology. The aims of this study were to gain insights into thermoassociative gel formation and to improve the understanding of the relationships between copolymer structure and gel elasticity.

Temperature-responsive copolymers undergo temperature-triggered chain contraction [7–9] when the solution temperature reaches the lower critical solution temperature (LCST). They can, through thermoassociation, form macromolecular micelles. The seminal work in the context of concentrated solutions of thermoassociative copolymers was conducted by Hourdet et al. [4,5,10–14]. Their copolymers were prepared using conventional free-radical polymerization and often contained NIPAm. Structural variations studied by those workers included anionic copolymers [5,11,15] as well as cationic copolymers [4]. The anionic copolymers contained a negatively charged backbone and PNIPAm side chains [5]. The cationic copolymer consisted of a linear copolymer with

---

[*] Corresponding author.
E-mail address: brian.saunders@manchester.ac.uk (B.R. Saunders).

0032-3861/$ – see front matter © 2009 Elsevier Ltd. All rights reserved.
doi:10.1016/j.polymer.2009.01.035

cationic and NIPAm units along the backbone [4]. The LCST of that system was a function of copolymer composition. It has been established that a macromolecular structure with a charged backbone and groups that can associate to form physically crosslinked microdomains is an ideal candidate for reversible and controlled gel formation [14]. In our case, the positively charged backbone prevents complete temperature-triggered chain contraction, whilst the NIPAm segments of the side chains ensure that reversible crosslink formation occurs at temperatures greater than the LCST. The result is a space-filling network, or gel.

Thermoassociative copolymers have been previously studied by the Saunders group in the context of preparing temperature-triggered emulsion [3,16,17] and particulate dispersion gels [18]. In those studies an uncharged thermoassociative comb copolymer was used, which was PNIPAm-*co*-PEGMA, where PEGMA is poly(ethyleneglycol methacrylate). That copolymer [18] provided good surfactant-like behaviour and stabilized emulsions or particulate dispersions at room temperature. Aubry et al. investigated the rheological behaviour of CMC-*g*-PNIPAm graft copolymers [19]. (CMC is carboxymethyl cellulose.) Chitosan containing PNIPAm grafts were studied by Seetapan et al. [6] In addition an extensive study of thermoassociation and gelation of hydrophobically modified PNIPAm copolymers was performed by Wintgens and Amiel [20].

In the present study we extend our original study [1] of PDMA^+_x-*g*-(PNIPAm$_n$)$_y$ in order to consider concentrated solution behavioural changes in detail. Unlike the other cationic thermoassociative copolymer systems [4] our graft copolymers have cloud point temperatures (T_{clpt}) that are not dependent on copolymer composition. Here, we investigate the structure–property relationships of PDMA^+_x-*g*-(PNIPAm$_n$)$_y$ copolymer solutions in more detail, especially in the context of gel elasticity. We show that it is possible to change and control the gel elasticity by changing copolymer concentration or copolymer structure. This is the first study of its type for cationic graft copolymers containing PNIPAm.

2. Experimental

2.1. Copolymer synthesis

The synthesis and characterization of the copolymers used in this work were described in detail earlier [1]. A brief description is given here (see Scheme 1). All reagents were purchased from Aldrich and purified with standard methods to remove the inhibitors and impurities before use. Water was of Milli-Q quality. The PDMA^+_x-*g*-(PNIPAm$_n$)$_y$ copolymers were prepared by aqueous ATRP using a macroinitiator (MI). The MIs were prepared by conversion of poly(DMA-*stat*-HEMA) (hydroxyethyl methacrylate) to a quaternarized, isobutyrate functionalized, version [1] using the method pioneered by Chen and Armes [21]. To prepare PDMA^+_x-*g*-(PNIPAm$_n$)$_y$, CuBr/PMDETA (*N*,*N*′,*N*″,*N*″-Pentamethyldiethylenetriamine) (1/1) and 0.25 mL of water were placed in a 100 mL two-neck reaction flask, which was then sealed. The flask was repeatedly evacuated and filled with Ar. Different ratios of NIPAm to MI (Table 1) were degassed as 6% (w/v) monomer solutions in water before being transferred to the reaction flask. The polymerizations were conducted for at least 40 min, then opened to air, and acetone immediately added to stop the reactions. The graft copolymers were purified by dialysis to remove Cu catalyst/ligand and any unreacted monomer. The purified copolymers were isolated by freeze-drying. The copolymer molar masses and compositions were estimated using GPC of poly(DMA-*stat*-HEMA) and ^{1}H NMR of the cationic graft copolymers [1]. (See Table 1.) We use abbreviations of the type MI2-PNIPAm20k to simplify copolymer identification. (The “20k” indicates the target molar mass for the PNIPAm arms.) That copolymer contained two positive charges per PNIPAm repeat unit on average.

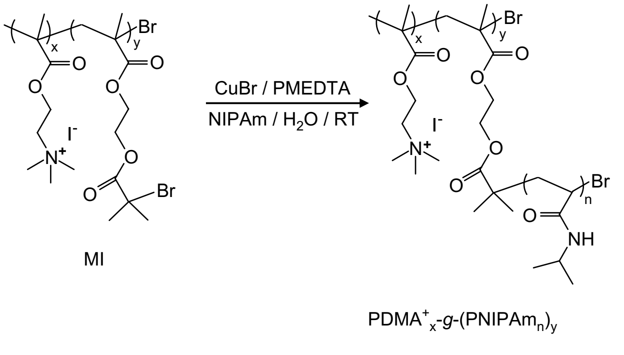

Scheme 1. Chemical structure of MI PDMA^+_x-*g*-(PNIPAm$_n$)$_y$

2.2. Linear PNIPAm synthesis

Linear PNIPAm was synthesized [1] using a similar method to that of the cationic graft copolymers *without* the use of a MI. The polymerization was conducted at room temperature using 6%(w/v) NIPAm aqueous solution.

2.3. Physical measurements

The determination of the cloud point temperature of the copolymer solutions (1 wt.%) was conducted with a Hitachi U-1800 spectrophotometer using a wavelength of 400 nm and thermostatic control. Gelation temperatures were determined using the tube inversion method. The internal diameters of the tubes were 17 mm. Dynamic oscillatory measurements were conducted using a strain-controlled rheometer (Gemini Advanced Rheometer, Bohlin Instruments). The parallel plate geometry was used. The upper plate diameter and gap were 20 mm and 0.1 mm, respectively. The strain used for these measurements was 10%. The operating temperature ranging from 25 to 50 °C was set and controlled by the temperature-controller. Dodecane was used as liquid seal to prevent water evaporation during measurement. Measurements were conducted in the linear viscoelastic region.

3. Results and discussion

3.1. Cloud points

The general structure of the MI-PNIPAm copolymers is shown in Scheme 1. Their compositions appear in Table 1. The structural variations explored in this work involve the effect of the number of charges per PNIPAm side chain (x/y ratio) and also the effect of PNIPAm chain length (n). The cloud point temperatures (T_{clpt}, Table 1) were determined from the points of inflection of the data shown in Fig. 1. The T_{clpt} values were indistinguishable from that for linear PNIPAm despite the large changes in the proportion of positively charged DMA$^+$ groups within the macromolecule. Thus, the copolymer composition can be varied substantially without affecting the LCST. This is generally what one would expect for a graft copolymer with a structure depicted in Scheme 1 since the PNIPAm chains and positively charged backbones are spatially separated.

3.2. Thermoassociative gelation of concentrated solutions

The temperature-triggered gelation of concentrated MI-PNIPAm solutions was investigated using tube inversion measurements (Fig. 2). A gel was judged to be present when inversion of the tube

Table 1
Preparation conditions, composition and properties of the copolymers.

Abbreviation	Composition[a]	x/y	M_n[b] (PD)	$[M]_o/[MI]_o$[c]	M_n[d]/g mol^{-1}	T_{clpt}/°C
MI1-PNIPAm20k	$PDMA^{+}_{23}$-g-$(PNIPAm_{195})_{23}$	1.0	6580 (1.44)	200	515,000	33.3
MI2-PNIPAm20k	$PDMA^{+}_{30}$-g-$(PNIPAm_{210})_{14}$	1.9	6480 (1.41)	200	348,000	33.6
MI3-PNIPAm20k	$PDMA^{+}_{37}$-g-$(PNIPAm_{195})_{12}$	3.0	7440 (1.34)	200	280,000	33.6
MI2-PNIPAm50k	$PDMA^{+}_{30}$-g-$(PNIPAm_{570})_{14}$	1.9	6480 (1.41)	500	918,000	33.3
PNIPAm		–	–	–	71,500[e]	33.4

[a] Composition is $PDMA^{+}_{x}$-g-$(PNIPAm_{n})_{y}$ based on the x, y and n values.
[b] Data for the respective poly(DMA-*stat*-HEMA) from GPC data.
[c] Concentration ratio of NIPAm to MI initially used.
[d] These values were calculated from ^{1}H NMR and GPC data (see ref. [1]).
[e] The polydispersity for this polymer was 3.6.

did not result in flow. The values of T_{gel} determined using this convenient method were obtained using some shear since the gels supported their own weight. We identify the gelation temperatures measured by tube inversion as $T_{gel(inv)}$ in the following discussion. It can be seen from Fig. 2(a) that the value for $T_{gel(inv)}$ corresponds to T_{clpt} for the MI2-PNIPAm20k solutions provided the copolymer concentration, C_{copol}, was at least 8 wt.% It can also be seen from the data that the minimum C_{copol} value for gelation is 5.0 wt.% by this method. Moreover, the $T_{gel(inv)}$ values for MI3-PNIPAm20k are the highest of all the systems studied (Fig. 2(a)). Because MI3-PNIPAm20k has the highest x/y value of all the copolymers studies here (Table 1) this shows that electrostatic interactions are important, and oppose gelation.

It can also be seen from the data shown in Fig. 2(b) that $T_{gel(inv)}$ increases as the PNIPAm side-arm length increases. Our earlier study showed that MI2-PNIPAm2k did not form gels when heated [1]. This shows that an optimum balance between the positive charge density of the backbone and ability of the PNIPAm side arms to associate is required for gel formation.

3.3. *Thermoassociative gel elasticity: effects of temperature and copolymer concentration*

The thermoassociative gelation process consists of temperature-triggered dehydration of the PNIPAm segments and concurrent formation of hydrophobic associative crosslinks. The spatial separation of the crosslinking points is crucial in determining whether or not a gel forms. The first network to form at the gel point will be very weak. It can be expected that the true T_{gel} value will be less than $T_{gel(inv)}$, unless C_{copol} is high, because the first-formed network will not have a sufficient number density of elastically effective chains to support the fluid mass upon tube inversion. In order to determine a more accurate value for T_{gel} dynamic rheology measurements were conducted for the MI2-PNIPAm20k system. Dynamic rheology is a sensitive, non-destructive, method for probing gel structure [22].

Fig. 3 shows dynamic rheological data for 5 wt.% MI2-PNIPAm20k solutions measured for a range of temperatures. For temperatures less than or equal to 33 °C the value for G' (storage modulus) is less than G'' (loss modulus) at all oscillation frequency (ω) values and $\tan\delta$ ($=G''/G'$) is therefore greater than 1.0. The

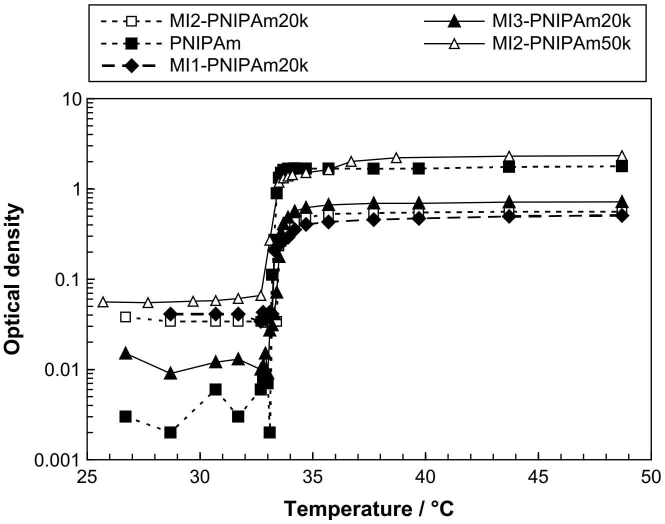

Fig. 1. Variation of optical density with temperature for various MI-PNIPAm copolymer solutions. Data for linear PNIPAm are shown for comparison.

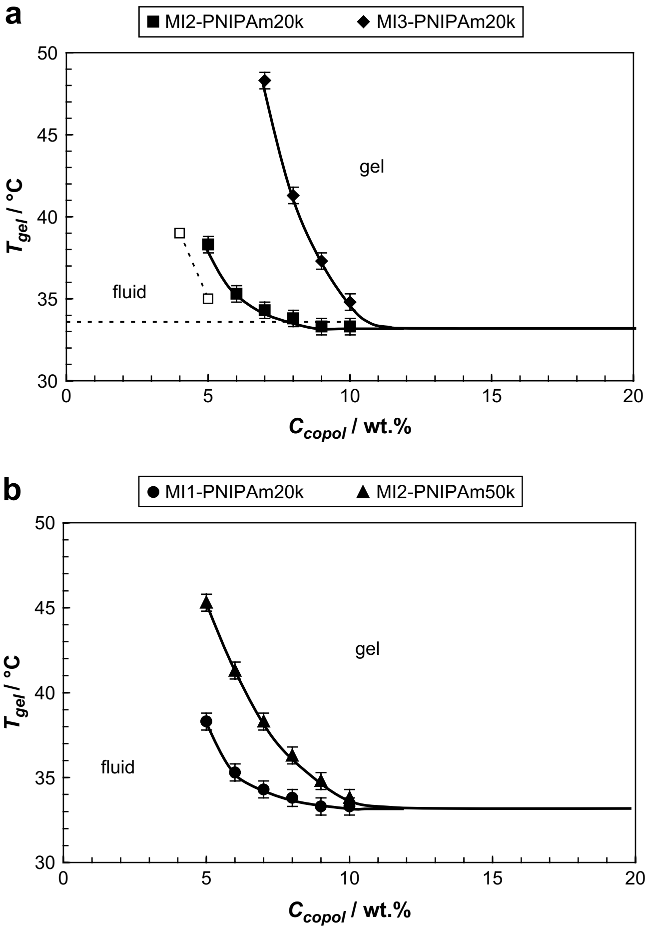

Fig. 2. Fluid-to-gel phase diagrams for MI-PNIPAm copolymer solutions. The open squares in (a) were obtained for MI2-PNIPAm20k using dynamic rheology data (below). The horizontal line in (a) is the value for T_{clpt} of MI2-PNIPAm20k.

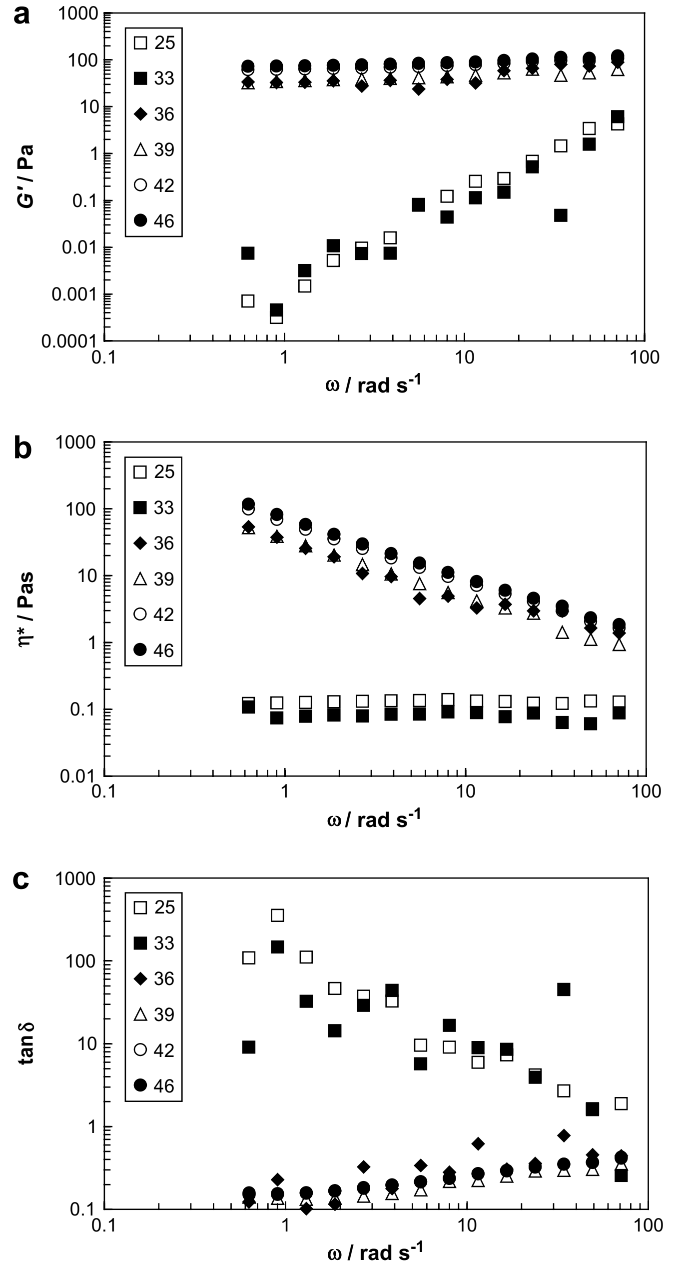

Fig. 3. Variation of (a) G', (b) η^* and (c) tan δ with ω for 5 wt% MI2-PNIPAm20k solutions measured over a range of temperatures (see legend).

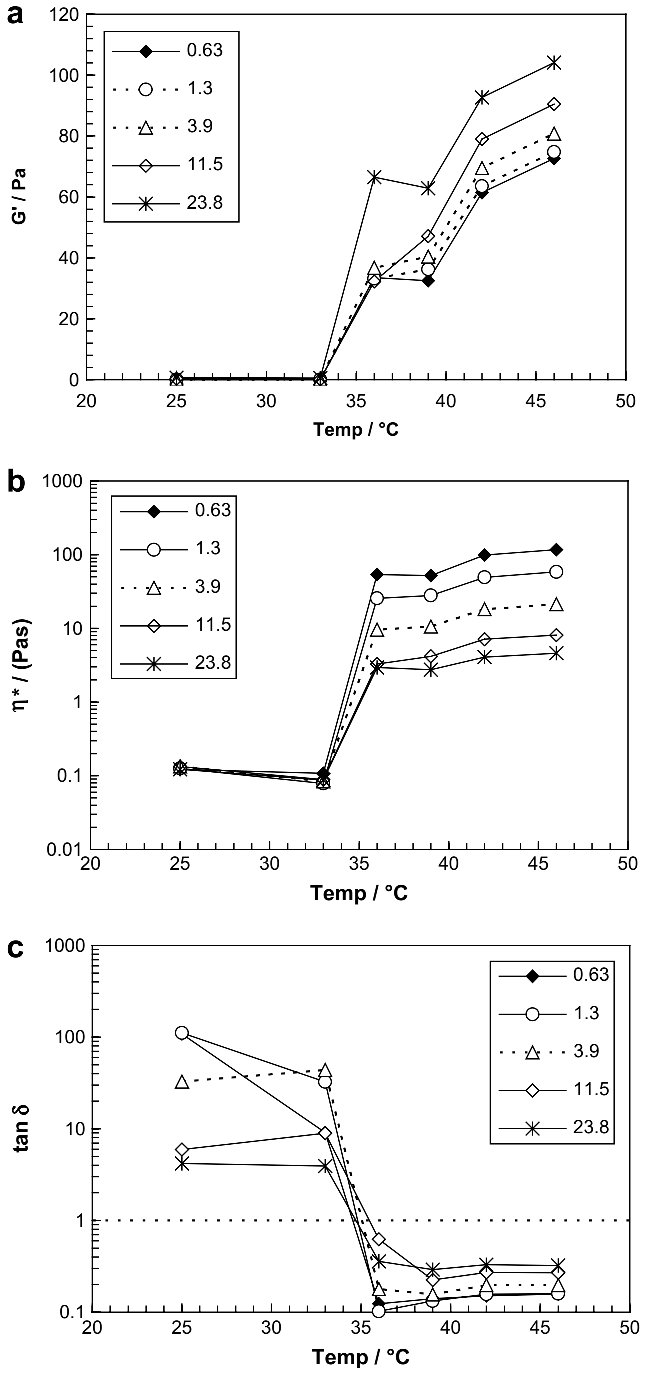

Fig. 4. Variation of (a) G', (b) η^* and (c) tan δ with temperature for 5 wt% MI2-PNIPAm20k solutions measured at different values for ω (see legend).

general form of the G' and tan δ vs. ω data are consistent with data reported for hydrophobically modified PNIPAm copolymer solutions [20] at temperatures below T_{clpt} and are indicative of a viscous fluid. At temperatures greater than or equal to 36 °C the behaviour changes considerably. It can be seen from Fig. 3(a) that G' increases substantially and becomes much less dependent on ω. The frequency-dependent behaviour for the dynamic viscosity (η^*, Fig. 3(b)) becomes a decreasing function of ω. Furthermore, the absolute values for tan δ are less than 1.0 at temperatures greater than or equal to 36 °C and the gradient of the log(tan δ) vs. log ω curve becomes positive (Fig. 3(c)) with a reduced dependence on ω. These data are evidence of thermoassociative gel formation. They are comparable to what has been reported for chitosan-g-PNIPAm copolymers [6] at temperatures greater than T_{clpt}. The data shown in Fig. 3 could not be fitted using the Maxwell model [22]. This implies that a distribution of relaxation times is present at temperatures greater than or equal to 36 °C, which is consistent with a range of structural configurations that comprise the associative crosslinks of the gelled state.

In order to probe gel formation in more detail the variation of G', tan δ and η^* was plotted as a function of temperature for a range of ω values (Fig. 4). Clearly, G' and η^* both increase abruptly at temperatures greater than 33 °C (Fig. 4(a) and (b)). The data for tan δ (Fig. 4(c)) can be used to determine an accurate value for T_{gel} using the criteria that at this point G' is greater than or equal to G'', i.e., tan $\delta \leq 1.0$. The gel point can therefore be identified by the temperature at which tan $\delta = 1.0$ across the frequency range probed. This temperature, which is defined here as the rheological gelation temperature ($T_{gel(rheol)}$), is 35.0 ± 0.5 °C from the data shown in Fig. 4(c). This is close to the T_{clpt} value for MI2-PNIPAm20k of 33.6 °C (Table 1). It is reasonable that T_{gel} should be close to T_{clpt} because thermoassociation leading to inter-chain crosslinking is a prerequisite for network formation. Seetapan et al. [6] measured gelation temperatures for their chitosan–PNIPAm copolymers that were similar to the respective cloud points.

An additional criterion for the gel point is that tan δ is independent of frequency. This is the Winter–Chambon criterion for gelation [23,24]. It can be seen from Fig. 3(c) that there is a change of sign for the gradient of tan δ with ω at temperatures between 33 and 36 °C. The gradient is negative at temperatures less than 33 °C and positive at temperatures greater than or equal to 36 °C. It is reasonable to suggest that tan δ would be independent of ω in the vicinity of 35.0 ± 0.5 °C. The Winter–Chambon criterion appears to apply to the gel point identified above for this system.

The effect of C_{copol} on the viscoelastic properties of the gels was also investigated. Values for G', η^* and tan δ obtained using a range of ω values are shown as a function of C_{copol} in Fig. 5. It can be seen that G' is a strongly increasing function of C_{copol}. This is the first time that this relationship has been tested for thermoassociative polymers to our knowledge. Transient network theory [25,26] predicts a linear relationship between the elastic modulus and C_{copol}. However, the data from Fig. 5 indicate a greater than linear relationship between G' and C_{copol}. Durand and Hourdet [5] reported that the relative viscosity increased strongly with C_{copol} for PAA-*co*-PNIPAm at 60 °C. Curve fitting of the data from Fig. 5(a) revealed that the data generally follow the following empirical equation.

$$G' = 0.10 C_{copol}^{3.85} \tag{1}$$

The curve for equation (1) is shown in Fig. 5(a). It is also noted that η^* vs. C_{copol} data followed a related expression, $\eta^* = A \times C_{copol}^{3.85}$; where A was a function of C_{copol}. (See Fig. 5(b)).

It can be seen that many of the tan δ values for $C_{copol} = 2.0$ wt.% are greater than 1.0 (Fig. 5(c)). It is reasonable to conclude that this system is a fluid at 39 °C. Conversely, the data shown in Fig. 5(c) show that gels are present when C_{copol} is greater than or equal to 4.0 wt.% because tan δ is less than or equal to 1.0. Therefore, we can estimate a second $T_{gel(rheol)}$ value of 39.0 °C for $C_{copol} = 4$ wt.%. This datum point, as well as the one from the discussion for Fig. 4 above ($T_{gel(rheol)} = 35.0$ °C at $C_{copol} = 5$ wt.%) are also shown in the phase diagram on Fig. 2(a). From Fig. 2(a) it can be suggested that a true position of the first-formed network can be estimated from the $T_{gel(inv)}$ data by moving the $T_{gel(inv)}$ vs. C_{copol} boundary 1 wt.% toward lower values (i.e., moving the curve 1 wt.% to the left).

What is the significance of G' (or η^*) being a strongly increasing function of C_{copol} (e.g., equation (1))? The concentration dependence of the elastic modulus has been studied for hydrophilic ethoxylated urethane associative polymers by Annable et al. [27] Those systems provide a reasonable comparison for thermoassociative copolymer solutions. The main difference is that the relaxation times for chain segments to disengage from network junctions and their functionality are considerably larger for thermoassociative copolymer solutions (above T_{clpt}). Annable et al. [27] noted that the elastic modulus increased more than linearly with C_{copol} and attributed this to topological changes involving entanglements. They argued that as C_{copol} increased the proportion of loops within the networks decreased. A decrease in the concentration of elastically ineffective loops for MI2-PNIPAm20k solutions is also likely with increasing C_{copol}. Furthermore, the functionality of the associative crosslinks should also be an increasing function of C_{copol}. It is therefore reasonable to attribute the supra-linear dependence of G' with C_{copol} to topological changes.

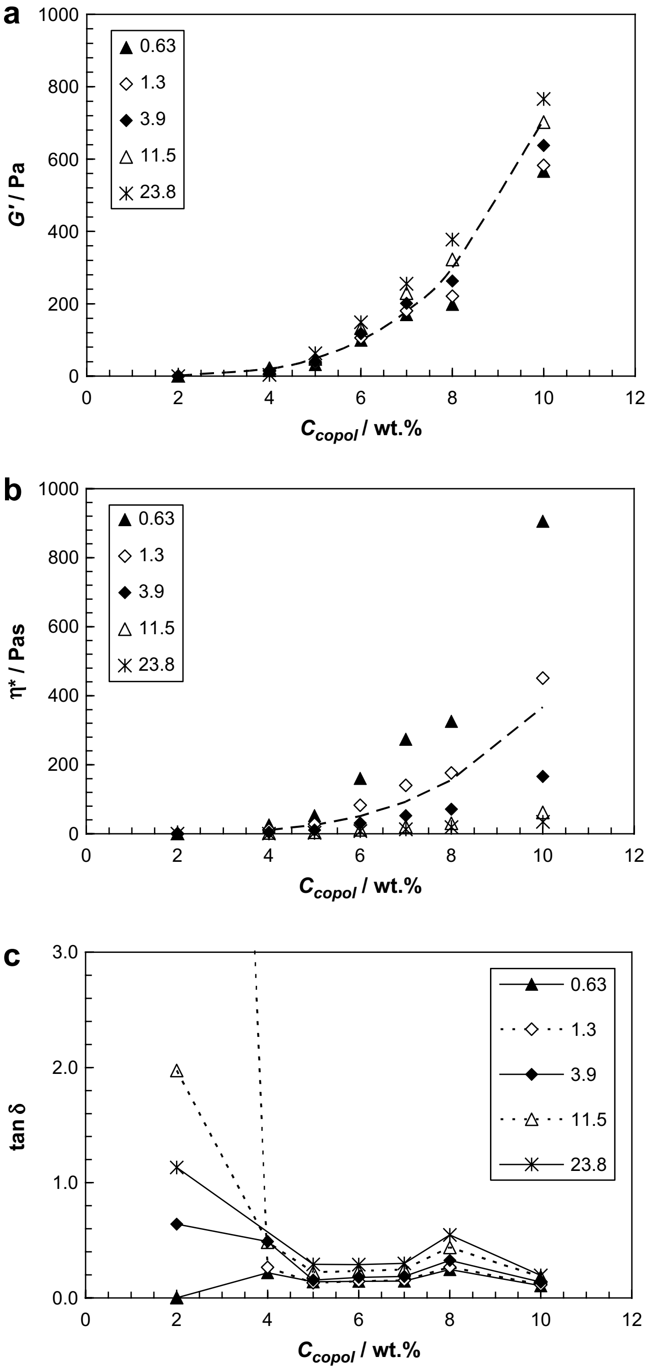

Fig. 5. Variation of (a) G', (b) η^* and (c) tan δ with C_{copol} for MI2-PNIPAm20k solutions at 39 °C. The data were measured at ω values shown in the legend. The long dashed curve in (a) is the fir from equation (1). The curve in (b) was obtained using $A = 0.0518$.

3.4. Thermoassociative gel elasticity: effects of salt and copolymer structure

We studied the effect electrostatic interactions on the rheological properties by investigating the effect of temperature using 5.0 wt.% MI2-PNIPAm20k solutions containing 0.1 M $NaNO_3$ (Fig. 6).

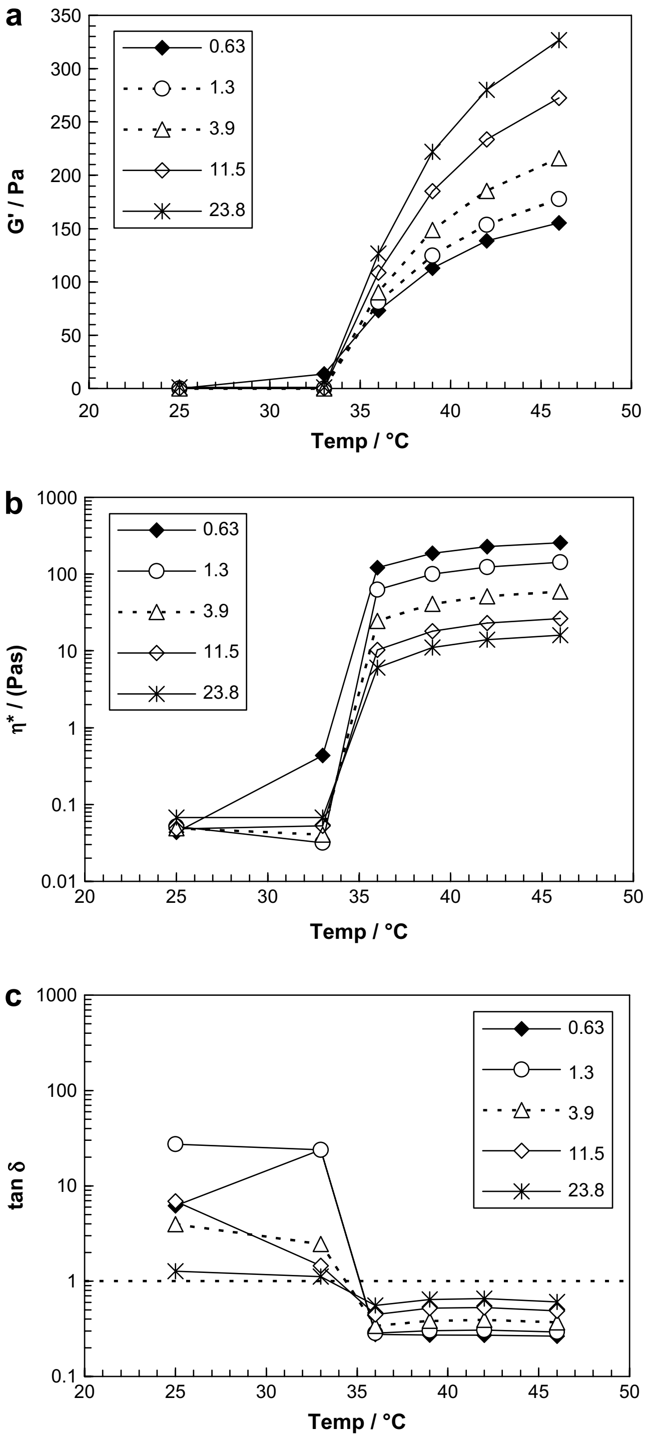

Fig. 6. Effect of added salt (0.1 M $NaNO_3$) on the variation of (a) G', (b) η^* and (c) tan δ as a function of temperature. The MI2-PNIPAm20k solution concentration was 5.0 wt%. These data should be compared with those shown in Fig. 4.

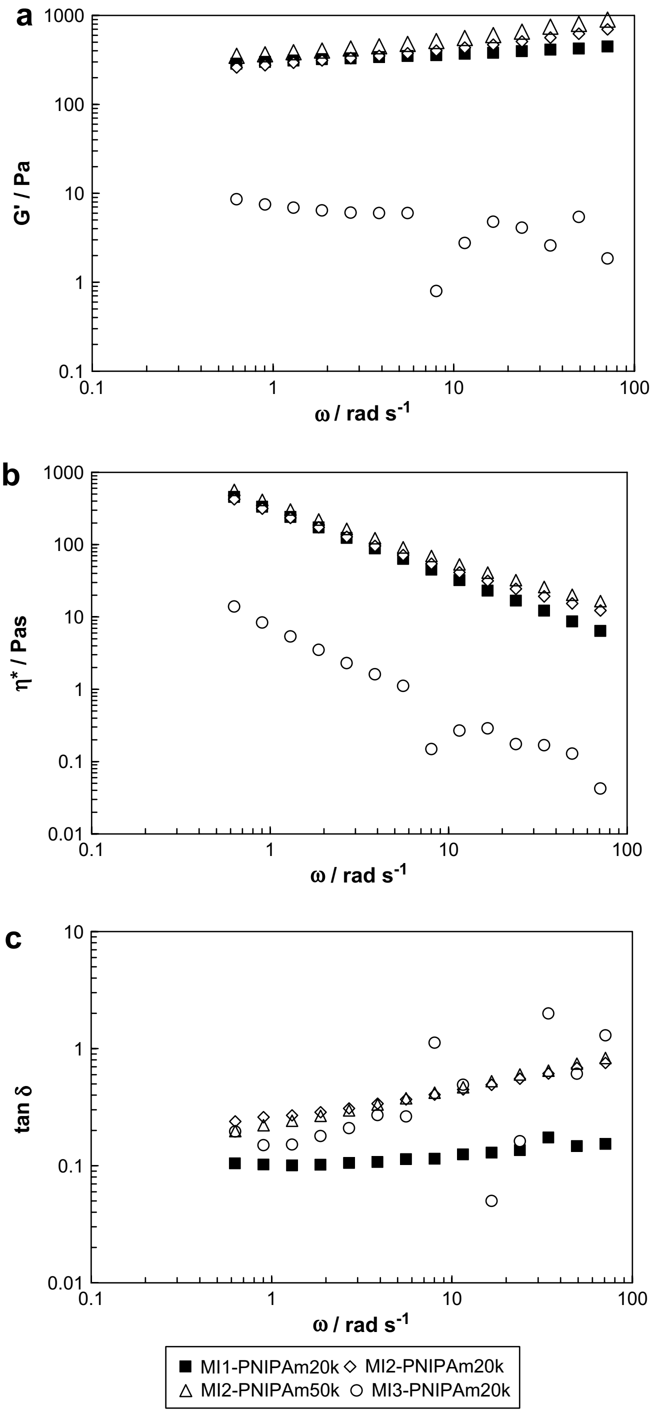

Fig. 7. Variation of (a) G', (b) η^* and (c) tan δ with ω for 8 wt% MI-PNIPAm solutions (see legend) measured at 45 °C.

These data should be compared to those measured in the absence of added salt (Fig. 4). The most noticeable changes are that the values for G' and η^* both increased substantially in the presence of 0.1 M $NaNO_3$. This is most pronounced for G' where the respective values are about three times greater. The temperature-dependence for tan δ has been less affected. The major increase in G' is indicative of a higher number density of elastically effective chains. This is attributed to electrostatic screening which allows closer approach of neighbouring MI2-PNIPAm20k chains and more effective association of PNIPAm side chains into crosslinks.

The effect of copolymer structure on the viscoelastic properties was also investigated. Fig. 7 shows the variation of G', η^* and tan δ with ω at 45 °C for 8 wt.% solutions of all the MI-PNIPAm copolymers (Table 1). This temperature was chosen because it resides well inside the gel regime of the respective phase diagrams (Fig. 2). We first consider the effect of positive backbone charge to PNIPAm side-arm ratio (x/y ratio). It can be seen from Fig. 7(a) and (b) that the frequency dependence of G' and η^* for MI1-PNIPAm20k and MI2-PNIPAm20k is similar. However, the copolymer with the highest x/y ratio, MI3-PNIPAm20k, has the lowest G' and η^* values. This is consistent with the higher $T_{gel(inv)}$ for that system (Fig. 2(a)) and can be attributed to greater electrostatic repulsion between neighbouring copolymer chains. This opposes thermoassociation of PNIPAm chains and reduces the number density and strength of the hydrophobic crosslinks.

An interesting observation from the data shown in Fig. 7 is that $\tan\delta$ has the lowest dependence on ω for MI1-PNIPAm20k. This is the system with the lowest x/y value (Table 1). For the other systems larger gradients for the $\log(\tan\delta)$ vs. $\log\omega$ plots are evident. (The same trend was evident at 39 °C – not shown.) This result implies that the associative crosslinks within the MI1-PNIPAm20k gels have the longest lifetimes with respect to $1/\omega$. MI1-PNIPAm20k (at $C_{copol} = 8$ wt.%) appears to provide an optimum balance between chain extension (due to the charged backbone) and inter-chain crosslinking (due to PNIPAm association).

The effect of PNIPAm side-arm length was also studied using the MI2-PNIPAm50k system (Fig. 7). Interestingly, there was no discernable difference between the rheological properties of this system and MI2-PNIPAm20k. This implies that the additional PNIPAm present with MI2-PNIPAm50k did not contribute to the network strength. It follows that only a fraction of the PNIPAm present within the MI-PNIPAm gels is actively involved in the network crosslinks. A significant fraction of the groups do not contribute to elasticity. Implicitly this would suggest the presence of a significant proportion of loops. This is consistent with conclusions from related work for PAA-*g*-PNIPAm copolymers [11]. One can see these results as an indication that the chain length between associative crosslinks or entanglements depends on the morphology of the aggregate which in turn is controlled by copolymer structure and C_{copol} for thermoassociative copolymer solutions.

Finally, it is noted that concentrated MI2-PNIPAm2k solutions do not form gels when heated [1]. It is therefore apparent that a minimum PNIPAm side-arm length (greater than 2k) is required for network formation. In view of the present study PNIPAm20k appears to have an optimum side-chain length for providing a low $T_{gel(inv)}$ value and strong gels.

The explanations presented above envisaged gels that consisted of elastically effective chains between associative crosslinks. There is, however, an alternative explanation for the gel structures which should also be noted. The thermoassociative gels could occur as a consequence of colloidal gelation (vitrification) where non-entangled objects, which we may assume are roughly spherical, aggregate due to hydrophobic effects (gelation). For those systems one would also expect a non-linear dependence of G' on C_{copol}, which has been observed for crosslinked Pluronic nanoparticles [28]. For the latter system entanglements were absent. A clear distinction between the structures responsible for our gels (elastically effective chains cf. vitrification) would require small-angle scattering data and is beyond the scope of the present work.

4. Conclusion

In this work we have investigated the thermoassociative behaviour of MI-PNIPAm copolymer solutions. Unlike other reports, the present system enabled the copolymer structure to be modified without changing the LCST. This simplified the interpretation of relationships between macromolecular structure and gel formation and properties. The values for G' and η^* for the MI2-PNIPAm20k gels scale with $C_{copol}^{3.85}$, which should allow gel property tuning. The most efficient systems in terms of their ability to form gels at low C_{copol} values were MI1-PNIPAm20k and MI2-PNIPAm20k. The elasticity of the gels, as judged by G', was strongly dependent on electrostatic interactions. Decreasing the repulsion between neighbouring cationic backbones, by adding 0.1 M $NaNO_3$, increased G' and η^* substantially. The MI3-PNIPAm20k system contained the highest proportion of positive charge and gave the lowest G' values. The data showed that a significant proportion of PNIPAm units are not directly involved in network formation. This implies that there is considerable potential for improving the elasticity of thermoassociative gels by further optimization of the copolymer structure. Gel formation and elasticity of the gels for these graft cationic copolymers are governed by a balance between electrostatic repulsion involving the backbone positively charged segments and temperature-triggered hydrophobic association between PNIPAm side chains. The copolymers investigated in this work may provide potential application as rheological control additives for anionic dispersions. They may also be of use in studies involving injectable gels for soft tissue repair [29] because the transitions' temperatures are between room temperature and body temperature.

Acknowledgements

BRS gratefully acknowledges the EPSRC (EP/E001319/1) for funding this work.

References

[1] Liu R, De Leonardis P, Cellesi F, Tirelli N, Saunders BR. Langmuir 2008;24:7099.
[2] Liu R, Cellesi F, Tirelli N, Saunders BR. Langmuir 2009;25:490.
[3] Alava C, Saunders BR. Langmuir 2004;20:3107.
[4] Bokias G, Hourdet D, Illiopoulos I. Macromolecules 2000;33:2929.
[5] Durand A, Hourdet D. Macromol Chem Phys 2000;201:858.
[6] Seetapan N, Mai-ngam K, Plucktaveesak N, Sirivat A. Rheol Acta 2006;45:1011.
[7] Chen X, Qi Z, Huang Y, Pelton R, Ghosh R. Adv Mater Res 2008;47–50:1311.
[8] George CA, Alexander C. J Am Chem Soc 2007;129:11014.
[9] Idziak I, Avoce D, Lessard D, Gravel D, Zhu XX. Macromolecules 1999;32:1260.
[10] Durand A, Hourdet D. Polymer 2000;41:545.
[11] Hourdet D, Gadgil J, Podhajecka K, Badiger MV, Brulet A, Wadgaonkar PP. Macromolecules 2005;38:8512.
[12] Hourdet D, L'alloret FL, Durand A, Lafuma F, Audebert R, Cotton J-P. Macromolecules 1998;31:5323.
[13] L'Alloret F, Hourdet D, Audebert R. Colloid Polym Sci 1995;273:1163.
[14] L'Alloret F, Maroy P, Hourdet D, Audebert R. Revue de l'Institut Français du Pétrole 1997;52:117.
[15] Durand A, Hourdet D. Polymer 1999;40:4941.
[16] Koh A, Prestidge C, Ametov I, Saunders BR. Phys Chem Chem Phys 2002;4:96.
[17] Koh A, Saunders BR. Chem Commun 2000;24:2461.
[18] Alava C, Saunders BR. J Coll Inter Sci 2006;293:93.
[19] Aubry T, Bossard F, Staikos G, Bokias G. J Rheol 2003;472:577.
[20] Wintgens V, Amiel C. Macromol Chem Phys 2008;209:1553.
[21] Chen XY, Armes SP. Adv Mater 2003;15:1558.
[22] Goodwin JW, Hughes RW. Rheology for chemists: an introduction. Cambridge: RSC Press; 2000.
[23] Winter HH. Polym Eng Sci 1987;27:1698.
[24] Winter HH, Chambon F. J Rheol 1986;30:367.
[25] Green MS, Tobolsky AV. J Phys Chem 1946;14:80.
[26] Tanaka F, Edwards SF. Macromolecules 1992;25:1516.
[27] Annable T, Buscall R, Ettelaie R, Whittlestone D. J Rheol 1993;37:695.
[28] Missirlis D, Hubbell JA, Tirelli N. Soft Matter 2006;2:1067.
[29] Freemont AJ, Saunders BR. Soft Matter 2008;4:919.